Pergamon
www.elsevier.com/locate/asr

Adv. Space Res. Vol. 27, No. 4, pp. 675–680, 2001

Printed in Great Britain
0273-1177/01 $20.00 + 0.00

PII: S0273-1177(01)00109-0

COSMIC-RAY ELECTRON FLUX FROM 10 TO 100 GEV MEASURED BY THE BETS INSTRUMENT

S.Torii[1], T.Tamura[1], N.Tateyama[1], K.Yoshida[1], T.Ouchi[1], J.Nishimura[2] T.Yamagami[2], Y.Saito[2], H.Murakami[3], T.Kobayashi[4], Y.Komori[5], K.Kasahara[6], and T.Yuda[7]

[1] *Faculty of Engineering, Kanagawa University, Yokohama 221-8686, JAPAN*
[2] *Institute of Space and Astronautical Science (ISAS), Sagamihara 229-8510, JAPAN*
[3] *Department of Physics, Rikkyo University, Tokyo 171-8501, JAPAN*
[4] *Department of Physics, Aoyama Gakuin University, Tokyo 157-8572, JAPAN*
[5] *Kanagawa Prefectural College, Yokohama 241-0815, JAPAN*
[6] *Shibaura Institute of Technology, Omiya 330-8570, JAPAN*
[7] *Institute for Cosmic Ray Research, University of Tokyo, Kashiwa 277-8582, JAPAN*

ABSTRACT

New measurements of the electron flux from 10 to 100 GeV were carried out with the BETS (balloon-borne electron telescope with scintillating fibers) instrument. The detector is an imaging calorimeter consisting of scintillating-fiber belts of 36 layers (each 280 mm wide) and the 8 plates of lead (each 5mm thick). Rejection of the background protons was performed at an efficiency of ~2000 using the shower imaging capability with high granulation. The observed electron flux around a few 10 GeV is consistent with the recent results reported by the HEAT group. Comparing the flux with theoretical expectations from a diffusion model, the best fit is obtained for the model of a diffusion coefficient of $2 \times 10^{28}(E/GeV)^{0.3}$ cm^2/sec for the SN rate of once per 30 years in the Galaxy.

INTRODUCTION

Major purposes in cosmic-ray studies are to make clear the origin, the acceleration mechanism and the propagation properties inside the Galaxy. Along this line many efforts have been expended to observe a precise spectrum of the various components in cosmic rays. Electrons in cosmic rays have unique features compared with other components since they are related directly to a number of significant astrophysical questions, such as the nature and distribution of the sources in the Galaxy, and the characteristics of cosmic-ray propagation in the Galactic disk and halo.

During propagation through the Galaxy from the sources, high-energy electrons lose their energy rapidly by synchrotron radiation in the Galactic magnetic field and the inverse Compton process on the interstellar photon field. The energy-loss rate is proportional to the square of the energy; the life time becomes shorter in proportion to the inverse of energy. This brings also a steeping of the observed energy spectrum during the propagation in the Galaxy.

In order to clarify the astrophysical aspects of the spectral shape, theoretical studies have recently been carried out by solving the diffusion equation in the Galaxy (Nishimura et al. 1980; Atoyan et al. 1995; Nishimura et al. 1997; Pohl and Esposito 1998), and also by using a code to compute self-consistently the other components (Moskalenko and Strong 1998). From these calculations, many important theoretical aspects were derived for the energy spectrum.

However, the observed spectrum still could not meet the requirements of accuracy to define the parameters. The reason the electron measurements still can not have sufficient accuracy, in spite of so many observations during last ~ 30 years, is mainly due to their low intensity (~ 1 % of protons) which requires, in particular at high energies, rather large (and heavy) detectors with the capability of effective discrimination against the proton-induced background.

Many novel detectors have been invented to overcome the difficulty by using a combination of an electromagnetic calorimeter and a device for an independent particle identification, such as a gas Cherenkov counter (Müller and Meyer 1973), transition radiation detector (Prince 1979; Tang 1984; Müller and Tang 1987), magnet spectrometer (Buffington et al. 1975; Golden et al. 1984; Golden et al. 1994). Recently, advanced detectors for measuring positrons separately from negative electrons have been constructed by a combination of a transition radiation detector (Barwick et al. 1997) or a Ring Imaging Cherenkov(RICH) detector (Boezio et al. 2000) with a system of magnet spectrometer and calorimeter.

Electron measurements at higher energies above 100 GeV have uniquely been carried out by emulsion chambers (ECC). The merit of emulsion detector results from the excellent capability in electron identification and the large acceptance. The exposure factor of ECC has attained 7.7 m^2 day sr, which is larger than the other observations by nearly two orders of magnitude. The group has already achieved extension of the observed spectrum up to a few TeV (Kobayashi et al. 1999). However, it is not easy to detect electrons below a few 100 GeV because the event detection by naked-eye scanning is not available in such low energies due to the accumulation of background tracks. The exposure factor below 100 GeV is, therefore, less than 0.1 % of that in the TeV region. The observation of electrons from 10 GeV to several 100 GeV is still far from completion for detailed discussion of the acceleration and propagation of the electrons.

The Balloon borne Electron Telescope with Scintillating fibers (BETS) has been developed as a detector which preserves the superior qualities of both electronic detectors and emulsion chambers. Namely, it can observe the details of shower starting points and shower profiles with a timing capability. Our primary aim of the new measurements with the BETS is to determine the energy spectrum of electrons in the energy region between 10 GeV and 100 GeV by applying the latest technology for electron selection, which was not used in previous detectors.

INSTRUMENT

The BETS instrument consists of a shower detector incorporating an imaging calorimeter and a trigger system, an electronics system, a data recording system and a telemetry system. Details of the telescope and the method of data analysis are presented in Torii et al. (2000). Study of the performance including an accelerator beam test at Super Proton Synchrotron(SPS) in CERN was also presented in Tamura et al. 2000. In Table 1, the basic performance is summarized.

Table 1.Instrument Performance Summary

Characteristics	Performance
Energy Range	10 GeV ~ a few 100 GeV
Geometric Factor ($\theta < 30^o$)	~ 320 cm^2 sr
Proton/Electron Discrimination	~ 2,000
Energy Resolution	14 % ~ 17 %
Angular Response	$0^o.8 \sim 1^o.3$
Total Weight	~ 320 kg
Power Consumption	130 W

Imaging Calorimeter

The calorimeter has an effective area of 28 cm × 28 cm, and it consists of 36 layers (18 in each of the orthogonal views) of scintillating fiber (SciFi) belts with lead plates of total depth of ~7 r.l. Each belt is composed of 280 round SciFi's (1 mm ϕ each) with one millimeter pitch. The total number of SciFi's is 10,080 (5,040 for each direction). The optical guides of fibers are made of clear fibers which have no efficiency to charged-particles in order to remove the noise. SciFi's outputs were observed with an image-intensified CCD camera. The CCD camera has an input window with a diameter of 10 cm and has a "shutter" function which is triggered by a gate signal (7 μs width) from the trigger system. The CCD data of 256 × 256 pixels is digitized with an 8-bit flash ADC and, recorded on EXB 8mm tape via a VME-bus memory buffer.

Event Trigger System

The trigger system was composed of three plastic scintillators which produce 3-fold coincidence for electrons and the trigger thresholds were set to distinguish charge. These scintillators were put at the top of detector (S_1), the depth of $\sim$ 2 r.l. (S_2) and the bottom (S_3), respectively. Each scintillator with a thickness of 1cm is viewed by a photomultiplier through a light guide.

The trigger thresholds are optimized to enhance the fraction of electrons in the triggered events by simulations. For the observation of electrons over 10 GeV and with a zenith angle smaller than 30 degrees, the highest proton-rejection power of $\sim$ 100 at 85% electron efficiency is achieved if we impose the numbers of particles observed in S_1, S_2 and S_3 be 0.7 $\sim$ 5, $\geq$ 10, and $\geq$ 40 (in units of single minimum ionizing particle of vertical incidence), respectively. The rejection power is enough to decrease the trigger rate during observation as low as $\sim$ 2 Hz.

Accelerator Beam Test

The detector performance was calibrated at accelerator beams. The energies cover from 5 GeV to 100 GeV for electrons; from 60 GeV to 250 GeV for protons. The energy resolution, the angular response and the detection efficiency were calibrated for electrons. The proton-rejection capability was examined at various conditions of beam energies, incident positions on the detector, and the incident angles. The detector was irradiated in the beams under the exactly same condition as the balloon experiment to estimate the real performance.

The energy of electromagnetic showers was measured by the pulse height at the bottom scintillators, S_3. As presented in Figure 1, the relation between the average pulse heights and the electron energies is nearly linear. The energy resolution was obtained by using a Gaussian fit to the pulse height distribution at each energy. The energy resolution is nearly constant, ranging from 14 % to 17 % in 10 -100 GeV. The angular resolution was obtained by measuring the angle between the incident beam and the shower axis reconstructed from the observed shower image. In Figure 2, we present the angular distributions at an incident angle of 15° for the electron beams. The distribution at each energy could be fitted by a Gaussian function. The angular resolution becomes better with increasing energies from 1.3 degrees at 10 GeV to 0.8 degrees at 100 GeV.

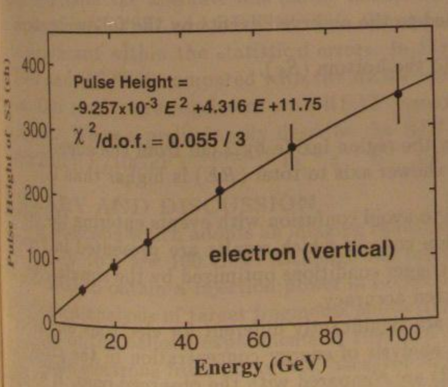

Fig. 1. Relation of electron energies and pulse heights (in ADC count) at the bottom scintillator, S_3, observed by the CERN-SPS beams. The error bars are standard deviations obtained by a Gaussian fit to the energy distribution.

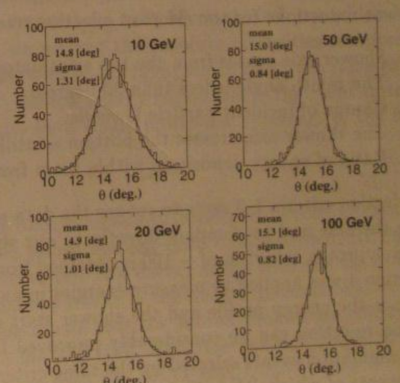

Fig. 2. Angle response of the fitted shower axis to the beam direction of electrons at each energy. The solid curve is a Gaussian distribution of the best fit to the data.

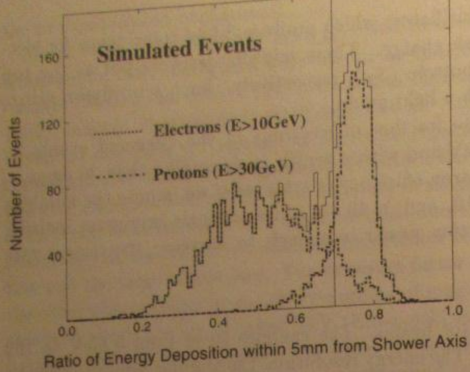

Fig. 3. Distribution of REs for the simulated proton and electron events after the "instrument trigger" (see text).

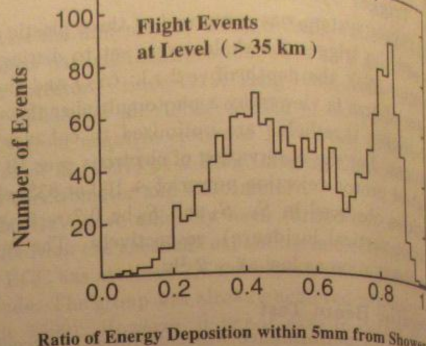

Fig. 4. Observed RE distribution by the flight events at an altitude over 35 km in BETS97. The events plotted here have been selected by the criteria of 1) to 3) in text.

BALLOON EXPERIMENT

Balloon Flights and Event Statistics

The instrument was launched in June, 1997 (BET97) and May, 1998 (BETS98) from Sanriku Balloon Center in Japan, and was flown in total for about 13 hours at an altitude above 34 km. A total of [illegible] events were collected as electron candidates, and the 628 events with energies above 12.1 GeV, well above the geometrical rigidity cut-off at 10 GV, have been obtained.

Electron Selection

Event reductions for the electron selection was applied to the observed events by the following steps.

1. Shower axis passes from the top scintillator(S_1) to the bottom (S_3).
2. The zenith angle is less than 30 degrees.
3. Charge of incident particle is single.
4. The shower axis crosses the bottom scintillotor in the region inside by 2 cm from the edge.
5. Ratio of energy-deposition within 5mm from the shower axis to total (RE) is higher than 0.7.

Selection criteria 1-3 serve to reduce the data sample to avoid confusion with events entering the detector from the side and to compare directly to our simulation code of which results are presented in Figure [illegible] Then, a proton rejection of ~ 100 is obtained from the trigger conditions optimized by the simulations. The criterion 4 was applied to measure energies in an expected accuracy.

Since the energy profile and the shower start depth are significantly different for electrons and protons, proton rejection can be considerably improved by the analysis of energy concentration in the criterion [illegible] The simulation events selected by the same criteria (1-3) are compared with the observed ones. If we select the events of which RE is higher than 0.7, the protons are rejected by 95% with 85 % electrons remaining. The observed RE distribution presented in Figure 4 is consistent with the simulated distribution. Finally we get a number for the rejection power closer to ~ 2000 for a cut of $RE > 0.7$.

Electron Flux at Top of Payload

The energy is determined for the electron candidates using the relation between pulse height in S_3 [illegible] energy derived from accelerator calibration tests. These same accelerator tests also determine the energy dependence on angle.

From the number of electron candidates (N_e), we have evaluated the electron numbers by correcting the proton contamination in the RE-cut. The number of electrons in $RE < 0.7$ ($N_{e/p}$) and that of protons

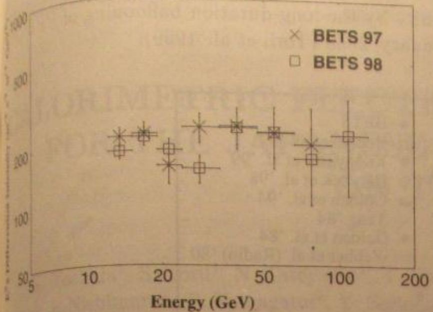

Fig. 5. Electron differential energy spectra (scaled by E^3) at the top of the atmosphere observed in BETS97 and BETS98. The errors are only statistical.

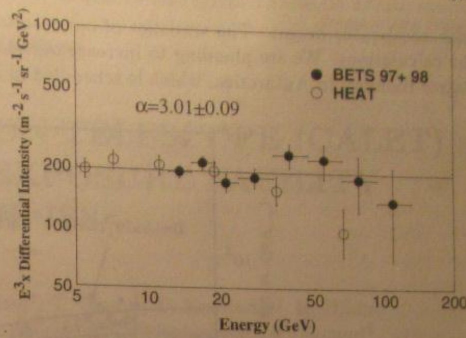

Fig. 6. Observed absolute differential energy spectrum for electrons and the comparison with the HEAT results. The solid line shows a power-law fit to the BETS results; $0.195(E/10\ \mathrm{GeV})^{-3.01}\ \mathrm{m^{-2}\ s^{-1}\ sr^{-1}\ GeV^{-1}}$.

$RE \geq 0.7$ ($N_{p/e}$) were estimated from the RE distribution obtained by the MC simulation. The number of electrons was given by $N_e - N_{p/e} + N_{e/p}$. This correction decreased the number of electrons by 11.5 %.

The electron flux at the top of the detector was calculated by the effective geometrical factor (detection efficiency × solid angle × area; $\epsilon\Omega A$) and the observed live times. The geometrical factor was obtained in each energy bin by the simulations, which are nearly constant, changing from ~ 280 cm² sr at 10 GeV to 290 cm² sr over 20 GeV. The fraction of live time to the total was 0.795 and 0.810 in BETS97 and BETS98, respectively.

ELECTRON FLUX AT TOP OF ATMOSPHERE

Our results of the absolute differential intensities of electrons are plotted in Figure 5, multiplied by E^3 for clarity, for BETS97 and BETS98. The discrepancies between these two observations are considered not to be significant within the statistical errors. In Figure 6, we present the absolute intensities composed of BETS97 and BETS98 compared with the HEAT results (Barwick et al. 1998) which cover the same energy region. Our results are consistent with HEAT, especially at the low energy region where the event statistics are higher. We can preliminarily describe the BETS results by a single power-law spectrum of the form: $0.195 \pm 0.014(E/10GeV)^{-3.01\pm0.09}\ \mathrm{m^{-2}\ s^{-1}\ sr^{-1}\ GeV^{-1}}$.

SUMMARY AND DISCUSSION

A new telescope which adopts an imaging calorimeter has been successfully developed to observe electrons from 10 GeV to a few 100 GeV. Although the full rejection power has not been demonstrated, BETS has the potential to obtain a rejection power in excess of 10^4 up to the TeV energy range with the use of more sophisticated analysis of target fragments and secondary hadron tracks in the nuclear interactions.

Analysis of the balloon experiments in 1997 and 1998 has shown that the shower profiles are efficient to discriminate electrons from the proton background up to a few 100 GeV. The observed flux above 10 GeV under ~ 5 g cm^{-2} of average residual atmosphere is consistent with the HEAT result.

In Figure 7, we present the BETS results with previous measurements (Webber et al. 1980; Tang 1984; Golden et al. 1984; Golden et al. 1994; Barwick et al. 1998; Kobayashi et al. 1999; Boezio et al. 2000) to compare with the calculation of two types of diffusion coefficients. Among several nearby sources listed in Nishimura et al. 1997, Monogem and Loop1 might have a significant contribution to the flux in the highest energy region. Our present results are consistent with the model of D=2.0 ×10^{28} (E/1 GeV)$^{0.3}$ cm²/s although it is difficult to answer which coefficient is preferable if we consider all of the present data.

It is known that the systematic discrepancy in the observations might result from two uncertainties, of the absolute energy calibration and the absolute detection efficiency of the instrument. We believe that our results are safe from both of them due to the simple structure of the detector and the calibration tests with accelerator beams. The statistics of our results is not enough to discuss the details of parame[…] the calculations. We are planning to increase our statistics by the long-duration ballooning of PPB (P[…] Patrol Balloon) in Antarctica, which is scheduled in January, 2003 (Torii et al. 1999).

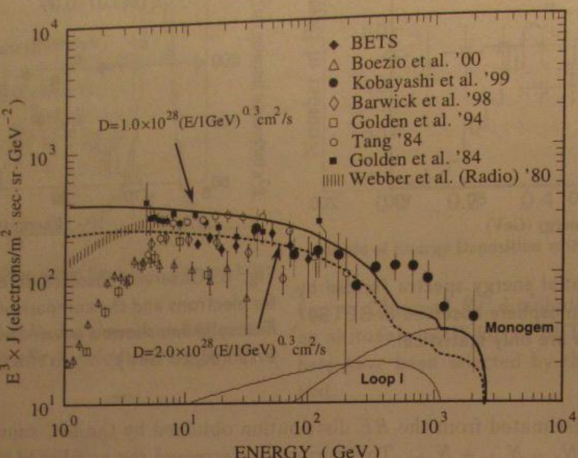

Fig. 7. Absolute differential energy spectrum for electrons and the comparison of calculated results by a diffu[…] model. The solid line shows the results calculated by a diffusion coefficient of $D=1.0\times10^{28}$ $(E/GeV)^{0.3}$ cm[…] with the individual contribution to the flux from the nearby sources (Loop1 and Monogem); the dashed is f[…] coefficient larger by a factor of two. In the latter, the flux from the nearby sources are not presented for simpli[…]

ACKNOWLEDGMENTS

We are indebted to the crew of the Sanriku Balloon Center, ISAS for the successful balloon flights. [...] express sincere thanks to Dr. L.Gatignon and the technical staffs in CERN for their help in the beam te[…] This work is partially supported by Grants-in-Aid for Scientific Research (A).

REFERENCES

Atoyan,A.M.,Aharanian,F.A.,and Völk,H.J.,*Phys. Rev.D* ,**52**,3265,1995
Barwick,S.W.,Beatty,J.J.,Bower,C.R.,Chaput,C.J.,Coutu,S.,et al.,*Nucl. Instru. & Meth.*,**A 400**,34,199[…]
Barwick,S.W.,Beatty,J.J.,Bower,C.R.,Chaput,C.J.,Coutu,S.,et al.,*Ap.J.*,**498**,779,1998
Boezio,M.,Carlson,P.,Francke,T.,Weber,N.,Suffert,M.,et al.,*Ap.J.*,**532**,653,2000
Buffington,A.,Orth,C.D.,and Smoot,G.F.,*Ap.J.*,**199**,669,1975
Golden,R.L.,Mauger,B.G.,Badhwar,Daniel,R.R.,G.D.,Lacy,J.L.,et al.,*Ap.J.*,**287**,622,1984
Golden,R.L.,Grimani,C.,Kimbell,B.L.,Stephens,S.A.,Stochaj,S.J.,et al.,*Ap.J.*,**436**,769,1994
Kobayashi,T.,Nishimura,J.,Komori,Y.,Shirai,T.,Tateyama,N.,et al.,*Proceedings 26th ICRC,Utah*, 3,6[…]
Moskalenko,I.V.,and Strong,A.W.,*Ap.J.*,**493**,694,1998,
Müller,D.,and Meyer,P.,*Ap.J.*,**186**,841,1973
Müller,D.,and Tang,J.,*Ap.J.*,**312**,183,1987
Nishimura,J.,Fujii,M.,Taira,T.,Aizu,E.,Hiraiwa,H.,et al.,*Ap.J.*, **238**,394,1980
Nishimura,J.,Kobayashi,T.,Komori,Y.,and Yoshida,K.,*Adv. Space Res.*,19,711,1997
Pohl,M.,and Esposito,J.A.,*Ap.J.*,**507**,327,1998
Prince,T.A.,*Ap.J.*,**227**,676,1979
Tamura,T.,Torii,S.,Yoshida,K.,Yamagami,T.,Murakami,H.,et al.,*Adv. Space Res.*,**26**,1397,2000
Tang,K.K,*Ap.J.*,**278**,881,1984
Torii,S.,Yamagami,T.,Yuda,T.,and K.Kasahara,*Adv. in Polar Upper Atmosphere Res.*, **13**,176,1999
Torii,S.,Tamura,T.,Tateyama,N.,Yoshida,K.,Ouchi,Y.,et al.,*Nucl. Instru. & Meth.*,**A 452**,81,2000
Webber,W.R.,Simpson,G.A.,and Cane,H.V.,*Ap.J.*,**236**,448,1980